

## Azimuthal Symmetry, Flow Dynamics, and Heat Transport in Turbulent Thermal Convection in a Cylinder with an Aspect Ratio of 0.5

Chao Sun, Heng-Dong Xi, and Ke-Qing Xia

*Department of Physics, The Chinese University of Hong Kong, Shatin, Hong Kong, People's Republic of China*

(Received 7 February 2005; published 12 August 2005)

We report an experimental study of flow dynamics and structure in turbulent thermal convection. Flow visualization, together with particle image velocimetry (PIV) measurement, reveal that the instantaneous flow structure consists of an elliptical circulatory roll and two smaller counterrotating rolls, and that the azimuthal motion of the quasi-2D instantaneous flow structure produces a time-averaged 3D flow pattern featuring two toroidal rings near the top and bottom plates, respectively. The apparently stochastic azimuthal motion of the flow structure, which generates a net rotation on average, is found to possess the characters of a Brownian ratchet. Using an artificially generated flow mode, we are able to produce a bimodal-Nu behavior and thus demonstrate that different flow states can indeed produce different global heat transport in a turbulent convection system.

DOI: [10.1103/PhysRevLett.95.074502](https://doi.org/10.1103/PhysRevLett.95.074502)

PACS numbers: 47.27.Jv, 05.65.+b, 44.25.+f

The Rayleigh-Bénard (RB) model, a fluid layer heated from below and cooled on the top, has become the paradigm for the thermal convection phenomenon, which plays a vital role in the dynamics of such systems as the Earth's atmosphere, oceans, and its mantle. A full understanding of this system thus not only is of fundamental interest but will also shed light upon a wide range of more complicated convection problems occurring in nature [1–3]. A central issue in the study of turbulent convection is to understand how turbulent flows transport heat across the fluid layer. Despite many experimental studies on the heat transport [4–8] and on the velocity field [9–13], a clear relationship between the two has not been established. Some recent measurements of the Nusselt number Nu, the dimensionless global heat flux, have found a bimodal-Nu behavior under apparently identical conditions and it was suggested that this might be caused by the system switching between different flow modes [14]. Multiflow modes were indeed observed in a numerical study [15]. The bimodal and even multimodal Nu behavior was later shown [16] to be present in data from a number of experiments and thus appears to be a more general phenomenon that does not seem to be correlated to any known experimental parameters or details of the apparatus used, which also makes the multistates explanation the most reasonable candidate. However, to our knowledge no direct link has ever been established between a specific flow mode and a particular value of Nu, either experimentally or numerically. It should be noted that the idea that global quantities such as Nu may depend on internal flow states is not at all obvious *a priori* and it has been previously suggested that global properties of turbulent convection may have an identical response to different local states [17]. A distinct feature of turbulent thermal convection in a closed box is a large-scale circulatory flow (LSC) [18]. Since its discovery, various aspects of the LSC have been extensively studied [19]. Still, the three-dimensional (3D) flow structure and the relationship between instantaneous and time-averaged flow field in this

system are not well understood. Therefore, understanding the 3D flow field and how the different flow modes affect global heat transport will shed light on the long-standing problem of RB convection.

This Letter reports an experimental study combining flow visualization, measurements of velocity field, and of Nu in a cylindrical convection cell of aspect ratio (cell diameter over height)  $\Gamma = 0.5$  filled with water. The cell has a diameter of 19.4 cm and a height of 38.8 cm, the plates are made of copper, and the sidewall is a Plexiglas tube with thickness 5 mm [8]. The flow visualization and Nu measurement was made in a thermostat (stability  $\pm 0.05$  °C) with its temperature matched to the mean fluid temperature in the cell and in Nu measurement the cell is further wrapped with thermal insulation. We first present the visualization study, conducted at the Rayleigh number  $Ra = 5.3 \times 10^{10}$  and at the Prandtl number  $Pr = 5.3$ . A Styrofoam bead (diameter  $\approx 1$  mm) attached to fishing lines (diameter = 0.18 mm) is used to visualize the azimuthal motion of the large-scale flow. The densities of the bead and the fishing line are such that the assembly is neutrally buoyant in the fluid. As shown in the upper-left inset of Fig. 1, two such assemblies, one near each conducting plate, were loosely reeled on a small stainless steel tube at the central axis of the cell. The beads have a distance of 2 cm from the sidewall so that they do not sense the predominantly vertical flows near the sidewall; rather, they follow the predominantly horizontal flows near the plates and thus indicate the orientation (or the azimuthal angle) of the vertical circulation plane of the LSC. Eight CCD cameras were used to record the motions of the beads, four focused on the top plate and four on the bottom; thus each covers a  $90^\circ$  azimuthal angular region. Outputs from the CCDs were recorded directly to computer hard disk at a rate of 0.7 frame/s and the images are analyzed to yield the time trace of the azimuthal angle  $\phi(t)$  of the two beads [20].

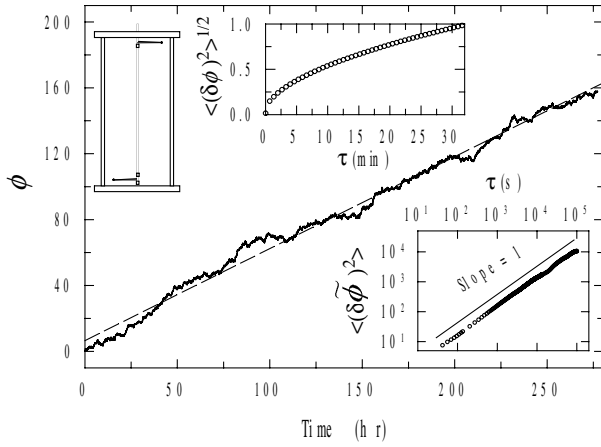


FIG. 1. Time trace of the azimuthal angle  $\phi(t)$  of the vertical circulation plane of the LSC. Top-left inset: schematic of bead-fishing line assembly for flow visualization. Top-right inset:  $\langle [\delta\phi(\tau)]^2 \rangle^{1/2}$  vs  $\tau$ . Lower inset: mean-square detrended angular displacement  $\langle [\delta\tilde{\phi}(\tau)]^2 \rangle$  vs  $\tau$ . All angular quantities in this figure are in units of  $2\pi$ .

Qualitative observations of the beads' movement show that the predominantly horizontal fluid flow near the two plates are always in opposite directions, confirming that the large-scale flow is in the form of a single roll [12]. We find that the azimuthal motion of the two beads is in the same direction and in phase, implying that the LSC moves azimuthally as a whole from top to bottom. As the two beads show essentially the same behavior, we present here results of the bottom bead only. Figure 1 shows the time trace of  $\phi(t)$  over a period of 277 h, where  $\phi(t)$  is defined as a continuous variable and positive is defined as anticlockwise when looked from top. The behavior of  $\phi(t)$  over the time scale of minutes reveals that the azimuthal motion of the LSC is quite erratic in both amplitude and direction. The wide range of dynamic scales of the azimuthal motion is also evidenced by the fact that the instantaneous angular velocity  $d\phi/dt$  can reach  $20^\circ/\text{s}$  while its average value is only  $2.5^\circ/\text{s}$ . A statistical measure of this dynamic behavior is  $\langle [\delta\phi(\tau)]^2 \rangle^{1/2}$ , where  $\delta\phi(\tau) \equiv \phi(t + \tau) - \phi(t)$ . This quantity gives the average time it takes the LSC to change the orientation of its vertical circulation plane by a certain angle. In the top-right inset of Fig. 1 we plot  $\langle [\delta\phi(\tau)]^2 \rangle^{1/2}$  as a function of  $\tau$ , which shows that it takes a relatively short period of time for the LSC to significantly change its orientation; a  $90^\circ$  change takes about 2 min, for instance. Over the time scale of hours, however, the azimuthal motion results in a net rotation, in the anticlockwise direction in this case. The dashed line in Fig. 1 represents the mean slope of  $\phi(t)$  which shows that the net rotation increases linearly with time; from it we obtain a net-rotation period of 107 min per revolution. Azimuthal motion over a large angular range has been observed in mercury in a  $\Gamma = 1$  cell [10] but not net rotations. We have tried to determine whether this phe-

nomon can be correlated to some experimental details by reassembling and releveling the convection cell, using different cells, restarting the convective motion, and varying the Ra. Invariably net rotation persists and is always in the same direction. To better understand this phenomenon, we subtract the linear increasing part (the dashed line) from  $\phi(t)$  itself and examine the displacement  $\delta\tilde{\phi}(\tau) = \tilde{\phi}(t + \tau) - \tilde{\phi}(t)$  of the detrended angular trace  $\tilde{\phi}(t)$ . The lower inset of Fig. 1 plots the mean-square detrended angular displacement  $\langle [\delta\tilde{\phi}(\tau)]^2 \rangle$  as a function of  $\tau$  on a log-log scale, which shows it has a linear dependence on  $\tau$ , similar to a Brownian motion. The histogram of  $\tilde{\phi}(t)$  is also found to be approximately Gaussian. Thus the azimuthal motion of the LSC appears to possess the characters of rectified Brownian motions, or Brownian ratchets [21], which have Brownian statistics with a nonzero mean displacement. We are not aware of any example of Brownian ratchet in a turbulent flow system, and in the present case it is unclear what is the ratchet potential [22] that generates the net angular displacement. We surmise it has to do with the Earth's coriolis force, which although too weak to drive the flow itself, somehow produces a bias when coupled to the stochastic dynamics of the turbulent flow. Note that net rotation is also observed recently in a  $\Gamma = 1$  cylinder but with a period of the order of 1 day [20,23].

The PIV system and the experimental parameters have been described previously [13], the only difference being in the present work each vector map comprises  $39 \times 78$  vectors. To prevent the distortion of the PIV images caused by the sidewall's curvature, a square-shaped jacket made of Plexiglas and filled with water is fitted to the outside of the sidewall [19]. Two measurements were made at  $Ra = 5.1 \times 10^{10}$  and  $Pr = 5.7$ ; in each a total of 40 000 vector maps are acquired, one sampled at 2 Hz (5.5 h duration) and the other 1 Hz (11 h). The obtained mean velocity field is the same in both cases. With the measured instantaneous field, we examine the velocity of a selected point ( $\sim 1$  cm

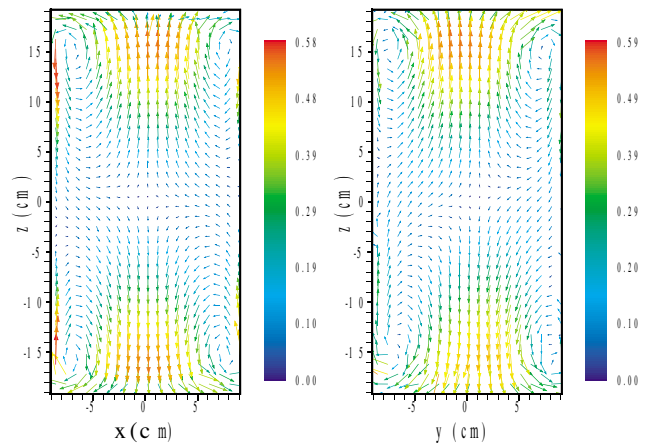


FIG. 2 (color online). Time-averaged velocity field measured in two vertical planes at  $90^\circ$  to each other in a leveled cell.

below the center of top plate) and found that its horizontal component fluctuates in a manner that is consistent with rotation, and over the measurement period of 11 h we did not see very fast switching between positive and negative values that would indicate sudden in-plane reversal of the LSC roll [11]. In the bead experiment, in-plane reversals would manifest as fast  $180^\circ$  azimuthal rotation of the LSC's circulation plane. The PIV result shows that reversals would be rare events which implies that most of the reorientations of the LSC's circulation plane observed in the bead experiment over a much longer period should be azimuthal rotations.

Figure 2 shows the mean velocity field in two vertical planes at  $90^\circ$  to each other, denoted as  $xz$  and  $yz$  planes, respectively. That the two panels in Fig. 2 look almost identical indicates that the mean velocity field in a  $\Gamma = 0.5$  cell is azimuthally symmetric. The four rolls in both panels show the existence of two tori near the top and bottom plates, which has been inferred in a numerical study [15] and in an experiment conducted in mercury [24], but their relation to the large-scale circulatory roll is not clear. Having shown the existence of the tori explicitly, we study how this flow structure arises from the instantaneous flow field by tilting the cell's vertical axis by about  $2^\circ$ , which locks the LSC in the azimuthal plane along the tilted direction [10,12]. Figure 3 shows the mean flow pattern in this plane (again denoted as  $xz$ ); it consists of an ellipse with two counterrotating rolls (CR) at the diagonally opposite corners. Combining this with results from leveled cell, we see that at any instant there are only the elliptical LSC and the CRs existing in a particular azimuthal plane.

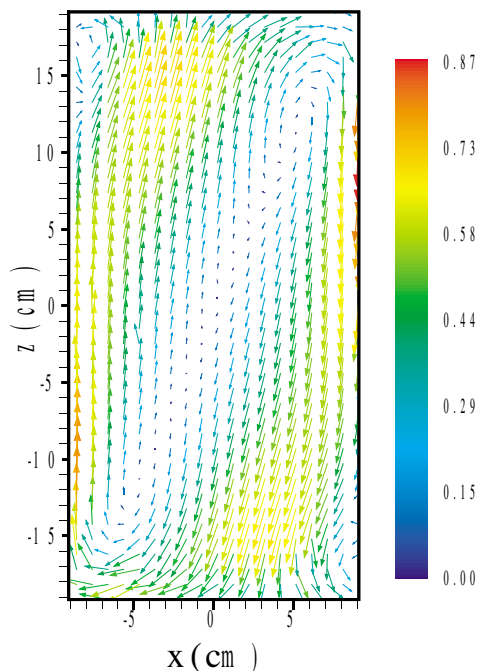


FIG. 3 (color online). Time-averaged velocity field measured in the  $xz$  plane in a cell tilted in the  $x$  direction.

After the LSC has rotated  $180^\circ$  azimuthally the flow pattern will be the mirror image of what it was before the rotation, so the ellipses will be canceled out in a time average but the CRs in the two images will appear in the four different corners. In fact, from instantaneous velocity maps measured in the leveled case we can identify patterns with the elliptical roll tilted in either diagonal directions and when these two types of patterns are added they give a velocity field similar to Fig. 2. This mechanism of the azimuthal motion of the instantaneous quasi-2D velocity field producing a 3D mean flow pattern featuring two tori is illustrated in Fig. 4. Based on the geometry of the cell, one might expect the instantaneous flow field to be azimuthally symmetric, such as fluid rises in the center and falls along the sidewall (or vice versa), which is clearly not the case. Recently it has been found in a  $\Gamma = 1$  cell that the orientation of the LSC plane has a preferred direction [25] so that even the time-averaged flow is not azimuthally symmetric in that case. The complicated azimuthal motion of the LSC roll found in both  $\Gamma = 0.5$  and  $\Gamma = 1$  cells [20,23] may be a manifestation that the system is attempting to restore its azimuthal symmetry in the time-averaged sense, and it succeeded for  $\Gamma = 0.5$  but not for  $\Gamma = 1$ , at least in the present range of Ra.

Measurement of the local heat flux has shown that heat transport across the cell is mainly carried by thermal plumes [26] and the majority of plumes are emitted within the band of the LSC [19]. On the other hand, because of the finite conductivity and finite heat capacity of the plates [27,28], once a plume is emitted from a spot on the plate that spot will be unable to emit plume again until its heat is replenished by thermal diffusion. In the present case the thermal diffusion time across the plate is about 180 s, while it is seen from the top-right inset of Fig. 1 that in a time interval of 120 s the circulation plane of the LSC has

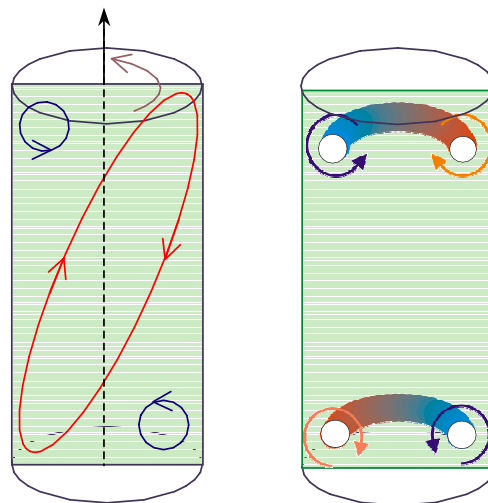


FIG. 4 (color online). Cartoon drawings of (a) instantaneous 2D flow pattern in a vertical plane that rotates azimuthally and (b) a vertical cut of the mean flow pattern.

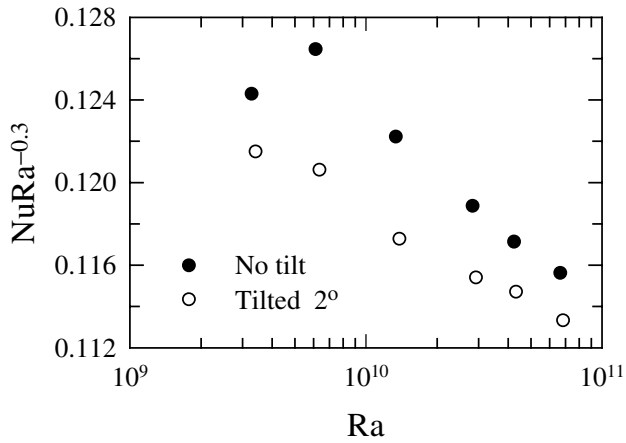


FIG. 5. Compensated Nu vs Ra for data measured in leveled and tilted cells, respectively, at  $Pr = 4.3$ .

rotated about  $90^\circ$  angle, so that the LSC now covers a very different region of the plate. This means that the majority of plume emissions can now occur without the need to wait heat replenishment to the old spot. The azimuthal sweeping of the circulation plane of the LSC thus should make heat transfer more efficient than the case when the LSC is locked in a particular orientation. To check this, we measured Nu over a 6 h period in both leveled and tilted cases, and Fig. 5 plots the result in compensated form (the 0.3 exponent is chosen for convenience), which shows the leveled case indeed has a larger Nu than the tilted one, with the difference varying from 2%–5%. To our knowledge, this is the first convincing demonstration that different flow modes can indeed give rise to different values of Nu. Our result also supports the conjecture that the Nu bimodality observed by Roche *et al.* [14] may be attributed to the system switching between different flow modes, these modes could be intrinsic to the system as was suggested [14–16], or they could be generated artificially by tilting the cell. Our finding is also consistent with the recent experiment by Chillà *et al.*, in which it was found that Nu in a tilted cell is indeed lower than in a leveled one and it was suggested that the difference is due to a transition from one-roll to two-roll flow states [29].

In summary, we have made an experimental study of the instantaneous and time-averaged flow fields and of the relation between different large-scale flow modes and the Nusselt number in a  $\Gamma = 0.5$  cylindrical cell. The instantaneous flow structure is found to consist of a single circulating roll spanning the height of the cell plus two small counterrotating rolls. As this quasi-2D instantaneous flow structure rotates azimuthally it traces out a time-averaged 3D flow pattern exhibiting two axisymmetric tori near the top and bottom plates, thus clarifying the relation between instantaneous and time-averaged flow

patterns. The apparently stochastic azimuthal motion of the large-scale circulatory roll, which produces a net rotation on average, appears to possess the characters of a Brownian ratchet. Using an artificially generated flow mode, we are able to produce a bimodal-Nu behavior and show that a particular value of Nu can be unambiguously associated with a specific large-scale flow mode in the convection cell. Our study thus demonstrates convincingly that the global quantity Nu does depend on the flow modes in the convection cell, which has been conjectured but not proven so far.

We thank G. Ahlers, P. Tong, B. Castaing, B. Chabaud, F. Chillà, B. Hébral, M. Rastello, and P. Roche for helpful discussions. This work was supported by the Hong Kong Research Grants Council (Project No. CUHK403003).

- 
- [1] E. D. Siggia, *Annu. Rev. Fluid Mech.* **26**, 137 (1994).
  - [2] S. Grossmann and D. Lohse, *J. Fluid Mech.* **407**, 27 (2000).
  - [3] L. P. Kadanoff, *Phys. Today* **54**, No. 8, 34 (2001).
  - [4] B. Castaing *et al.*, *J. Fluid Mech.* **204**, 1 (1989).
  - [5] J. J. Niemela *et al.*, *Nature (London)* **404**, 837 (2000).
  - [6] G. Ahlers and X. Xu, *Phys. Rev. Lett.* **86**, 3320 (2001).
  - [7] X. Chavanne *et al.*, *Phys. Fluids* **13**, 1300 (2001).
  - [8] K.-Q. Xia *et al.*, *Phys. Rev. Lett.* **88**, 064501 (2002).
  - [9] A. Belmonte *et al.*, *Phys. Rev. E* **50**, 269 (1994).
  - [10] S. Cioni *et al.*, *J. Fluid Mech.* **335**, 111 (1997).
  - [11] J. J. Niemela *et al.*, *J. Fluid Mech.* **449**, 169 (2001).
  - [12] X. L. Qiu and P. Tong, *Phys. Rev. E* **64**, 036304 (2001).
  - [13] K.-Q. Xia *et al.*, *Phys. Rev. E* **68**, 066303 (2003).
  - [14] P. E. Roche *et al.*, *Europhys. Lett.* **58**, 693 (2002).
  - [15] R. Verzicco and R. Camussi, *J. Fluid Mech.* **477**, 19 (2003).
  - [16] J. J. Niemela and K. R. Sreenivasan, *J. Fluid Mech.* **481**, 355 (2003).
  - [17] Z. A. Daya and R. E. Ecke, *Phys. Rev. Lett.* **87**, 184501 (2001).
  - [18] R. Krishnamurti and L. N. Howard, *Proc. Natl. Acad. Sci. U.S.A.* **78**, 1981 (1981).
  - [19] See, for example, H.-D. Xi, S. Lam, and K.-Q. Xia, *J. Fluid Mech.* **503**, 47 (2004), and references therein.
  - [20] H.-D. Xi, Q. Zhou, and K.-Q. Xia (to be published).
  - [21] C. S. Peskin *et al.*, *Biophys. J.* **65**, 316 (1993).
  - [22] R. D. Astumian, *Science* **276**, 917 (1997).
  - [23] E. Brown *et al.*, *Phys. Rev. Lett.* (to be published).
  - [24] Y. Tsuji *et al.*, *Phys. Rev. Lett.* **94**, 034501 (2005).
  - [25] C. Sun *et al.*, *Phys. Rev. E* (to be published).
  - [26] X.-D. Shang *et al.*, *Phys. Rev. Lett.* **90**, 074501 (2003).
  - [27] S. Chaumat, S. Castaing, and F. Chillà, *Advances in Turbulence IX, Proceedings of the 9th European Turbulence Conference*, edited by I. P. Castro, P. E. Hancock, and T. G. Thomas (CIMNE, Barcelona, 2002).
  - [28] R. Verzicco, *Phys. Fluids* **16**, 1965 (2004).
  - [29] F. Chillà *et al.*, *Eur. Phys. J. B* **40**, 223 (2004).